DEACTIVATION KINETICS FOR THE CONVERSION OF DIMETHYL ETHER TO OLEFINS OVER A HZSM-5 ZEOLITE CATALYST

Paula Pérez-Uriarte*, Ainara Ateka, Ana G. Gayubo, Tomás Cordero-Lanzac, Andrés T. Aguayo, Javier Bilbao

Department of Chemical Eng., University of the Basque Country (UPV/EHU). P.O. Box 644, 48080. Bilbao (Spain). (*) Corresponding author: paula.perez@ehu.es

ABSTRACT

A deactivation kinetic equation for the conversion of dimethyl ether (DME) to olefins (DTO process) has been established. The catalyst has been prepared with a HZSM-5 zeolite (SiO_2/Al_2O_3 ratio of 280) agglomerated with boehmite (mesoporous matrix of weak acidity). The experimental data have been obtained in an isothermal fixed bed reactor in a wide range of operating conditions: temperature, 573-673 K; space time, 0.2-6 g_{cat} h mol_C^{-1}; time on stream, 18 h; and different dilutions of DME (with He, methanol and water). The main cause of the catalyst deactivation is the coke deposition, being DME the principal precursor and the presence of water in the medium a key parameter in its attenuation. The kinetic model considers these effects and its use together with the kinetic model at zero time on stream results suitable to simulate the reactor over the whole range of operating conditions experimentally studied.

Keywords: DTO, olefins, HZSM-5 zeolite, kinetic model, coke, deactivation.

Highlights

- A kinetic equation for coke deactivation has been established.
- An 11 lumps kinetic model and the deactivation equation allow reactor simulation.
- Coke is heterogeneous and it is distributed in the matrix and the zeolite channels.
- DME concentration favors deactivation whereas water attenuates it.

Nomenclature

a	Activity.
C_C, C_{Ci}	Total coke content in the catalyst and content of *i* type coke, respectively, wt%.
d	Deactivation order.
E_d	Activation energy of the deactivation kinetic constant, kJ mol^{-1}.
E_{Ci}	Activation energy of each *i* coke fraction combustion, kJ mol^{-1}.
E_j	Activation energy of each *j* kinetic constant, kJ mol^{-1}.
F	Fischer distribution.
F_i, F_0	Molar flow rate of each *i* lump in the product stream and of DME in the feed, respectively, mol_C h^{-1}.
f_1, f_2	Parameters of the kinetic model at zero time on stream, defined in Eqs. (15 and 19) and (17 and 21), respectively.
f_{Ci}	Mass fraction of *i* type coke.
K_2	Equilibrium constant for the dehydration of methanol to DME, Eq. (24).
K_a, K_a^*	Parameter that quantifies the adsorption of (methanol + water) in the acid sites of the catalyst and the corresponding value at the reference temperature, respectively, atm^{-1}.
$K_{W,d}$, $K_{W,d}^*$	Parameter that quantifies the adsorption of water in the acid sites of the catalyst and the corresponding value at the reference temperature, respectively, h atm^{-1}.

k_{Ci}, k_{Ci}^* Kinetic constant for the combustion of each fraction of coke and the corresponding value at the reference temperature, respectively, $atm^{-1}\ h^{-1}$.

k_d, k_d^* Deactivation kinetic constant and its value at the reference temperature, respectively, $atm^{-1}\ h^{-1}$.

k_j, k_j^* Kinetic constant of *j* reaction step and the corresponding value at the reference temperature, respectively.

n_l, p, R_i Number of lumps, of experimental conditions and repetitions for each experimental condition, respectively.

OF_1, OF_2 Objective function to be optimized for the calculation of the kinetic parameters, Eqs. (4) and (30), respectively.

P Total pressure, atm.

p_i Partial pressure of *i* lump, atm.

P_{O2} Partial pressure of oxygen, atm.

r_i, $(r_i)_0$ Formation rate of *i* component at t and zero time on stream, respectively, $mol_{iC}\ g_{cat}^{-1}\ h^{-1}$.

r_j, $(r_j)_0$ Reaction rate of each *j* reaction step at t and zero time on stream, respectively, $mol_C\ g_{cat}^{-1}\ h^{-1}$.

s_a^2, s_e^2 Variance for the lack of fit and experimental error, respectively.

T, T^* Temperature and reference temperature, respectively, K.

W Mass of catalyst, g.

X Conversion.

$Y_{i,j}$, $Y_{i,j}^{*}$ Calculated and experimental values, respectively, of the composition of *i* lump at *j* condition, expressed as molar fraction referred to organic compounds, in C units.

Greek symbols

α Confidence level.

ΔH_a Apparent adsorption heat of (methanol+water), kJ mol^{-1}.

$\Delta H_{w,d}$ Apparent adsorption heat of water used in the deactivation equation, kJ mol^{-1}.

θ Term that quantifies the attenuation of the reaction rates by the adsorption of (methanol + water).

θ_d Term that quantifies the attenuation of the deactivation by the adsorption of water.

σ^2 Variance.

υ_i, υ_j Degrees of freedom for the model *i* and *j*, respectively.

υ, υ_a, υ_e Degrees of freedom for the lack of fit, experimental error and residual, respectively.

ω_i Weight factor for each *i* lump or compound.

Abbreviations of lumps and compounds

B, E, P Butenes, ethylene and propylene, respectively.

BTX, C_{5+}, O, Pa Aromatics (Benzene, Toluene, Xylenes), aliphatics with 5 or more carbon atoms, light olefins and C_2-C_4 paraffins, respectively.

D, M, W Dimethyl ether, methanol and water, respectively.

1. Introduction

Light olefins production from dimethyl ether (DME) is presented as an attractive route (DTO process) for complementing the production of olefins by steam cracking and catalytic cracking of naphtha, and as an alternative to the MTO process (methanol to olefins). The growing interest of the DTO process [1] is justified by the increase in the natural gas reserves [2] and the technological development of the DME synthesis in a single step, which has the following advantages over the methanol synthesis: i) the lower thermodynamic limitation, as methanol synthesis and its subsequent dehydration are performed in the same reactor (using a bifunctional catalyst) [3]; ii) the possibility to valorize syngas with low H_2/CO ratio, obtained (via gasification) from coal, biomass and wastes of the consumer society [4]; iii) the greater conversion of CO_2 (co-fed with syngas), which offers outstanding perspectives for the CO_2 valorization on a large scale [5-8].

DME conversion into light olefins is well known as the first stage of the methanol conversion, which is rapidly transformed in the MTO process in a mixture of DME, methanol and water, in equilibrium [9]. This fast dehydration occurs at the inlet of the reactor and consequently, the studies on the MTO process have been mainly focused on the following steps of oxygenates conversion (methanol and DME) into olefins and other hydrocarbons. This way, it is well known that the conversion of oxygenates into olefins occurs through the double cycle mechanism, although secondary reactions of by-product formation also take place, being remarkably significant the hydrogen transfer reactions for the formation of paraffins, aromatics, and the formation of coke, responsible for catalyst deactivation [10-13].

On the other hand, the rapid deactivation by coke deposition of the SAPO-34 catalyst in the MTO process has been widely studied [14-17], which is less pronounced in the

HZSM-5 zeolite catalysts [18,19]. This difference is justified by the characteristic three-dimensional porous structure of the zeolite, without boxes at the intersections, what facilitates the diffusion of coke precursors to the outside of the crystalline channels, avoiding the micropore blockage by coke.

The formation of olefins from DME in a catalytic reactor has been scarcely studied in the literature. Some authors point to the use of catalysts with severe shape selectivity such as SAPO-34 and SAPO-18 [20-22]. SAPO-34 undergoes on fast deactivation by the blockage of the micropores by coke [20,21], whereas SAPO-18 prepared (with a moderate acid strength) allows obtaining higher yields of olefins and shows more stability [22]. In addition, the moderate acidity of the HZSM-5 zeolite with a high SiO_2/Al_2O_3 ratio (SiO_2/Al_2O_3 = 280) allows to achieve a good compromise between activity, olefin selectivity and catalyst stability, as reported by other authors [23-25]. In a previous work using a catalyst prepared with this HZSM-5 zeolite [26], a kinetic model of 11 lumps has been established in order to quantify the effect of the reaction conditions (temperature, space time and feed composition) on the product distribution at zero time on stream.

Although the reaction schemes of DME and methanol conversion have the same individual steps (except for the methanol dehydration), the kinetic results reveal that the progress of the reaction is significantly higher in the DME conversion. This difference is explained by the faster transformation of DME to olefins than that of methanol [27,28] and by the higher water content in the reaction medium in the conversion of methanol, which mitigates the extent of the reaction [29,30].

On the other hand, it has been proven that DME conversion leads to a faster catalyst deactivation than that of methanol [24]. The lower water content in the reaction medium

than in methanol conversion has been proposed as the main reason of the faster deactivation due the key role of water in the attenuation of coke deposition [31,32].

The progress towards the implementation of the DTO process (or other processes with catalyst deactivation) requires a deactivation kinetic equation, which can be used for the design of the reactor together with the kinetic model at zero time on stream. In this work we propose a kinetic model for the transformation of DME to olefins, considering catalyst deactivation. Due to the scarcity of references in the literature on the deactivation kinetics of DME conversion, different kinetic equations established for the MTO process [33-36] has been used as a basis to develop that corresponding to the DTO process.

2. Experimental

2.1. Catalyst preparation and characterization

The commercial HZSM-5 zeolite (with SiO_2/Al_2O_3 molar ratio 280) has been supplied by Zeolyst International in ammonium form, and has been calcined at 843 K to obtain the acid form. Boehmite (Sasol Germany, 30 wt %) has been used as a binder, and a colloidal dispersion of α-alumina (Alfa Aesar, 22 wt %) as an inert filler (20 wt % in the catalyst) in order to agglomerate the zeolite in a mesoporous matrix. More details about the catalyst preparation procedure can be found elsewhere [23].

The physical properties of the fresh catalyst, determined by N_2 adsorption-desorption isotherms at 77 K (using Micromeritics ASAP 2000), are as follows: BET surface area, 301 $m^2\ g^{-1}$; micropore area, 95 $m^2\ g^{-1}$; micropore volume, 0.051 $cm^3\ g^{-1}$ and; pore volume, 0.45 $cm^3\ g^{-1}$. From the thermo-gravimetric measurement of tert-butylamine (t-BA) adsorption, a total acidity of 0.33 $mmol_{t\text{-}BA}\ g^{-1}$ at 373 K [24,37-38] has been

determined. By combining the thermo-gravimetric and calorimetric measurements, a uniform acid strength of 100 kJ $mol_{t\text{-}BA}^{-1}$ has been determined. The amount of coke deposited on the catalyst has been measured by temperature-programmed oxidation (TPO) in a TGA Q5000 thermobalance (TA Instruments). Prior to analysis the samples have been subjected to a N_2 stream for impurity removal and catalyst stabilization (50 cm^3 min^{-1} at 673 K, 20 min). After the stabilization the combustion experiment have been carried out with air (50 cm^3 min^{-1}) up to 848 K at 5 K min^{-1} and maintaining this temperature for 2 h in order to complete the combustion.

2.2. Reaction equipment, product analysis and operating conditions

The kinetic data have been obtained in an automated reaction equipment (Microactivity Reference of PID Eng&Tech, Madrid, Spain) connected online to a gas micro-chromatograph (Agilent CP 490) for the analysis of the reaction products [24]. The fixed bed reactor is made of 316 stainless steel and it is located inside a stainless steel covered cylindrical ceramic chamber. The bed consists of a mixture of catalyst and solid inert, carborundum (CSi), in order to ensure bed isothermicity and attain sufficient height under low space time conditions. The micro-chromatograph is provided with four analytical modules with the following columns: a molecular sieve (MS-5); Porapak Q (PPQ); Alumina; and 5CB (CPSIL).

The experiments have been carried out under different reaction conditions: temperature, between 573 and 673 K; total pressure, 1.5 atm; space time, 0.2-6 g_{cat} h mol_C^{-1}; time on stream, 18 h; feed, pure DME and diluted with He, water and methanol. Prior to each run, the DME transformation (unlike the methanol transformation) requires a conditioning treatment of the catalyst *in situ* (at 823 K with air for 2 h) to remove the water adsorbed on the acid sites of the catalyst [24].

Due to the large number of components, the composition of the product stream has been grouped into the following lumps: i) ethylene (E), ii) propylene (P), iii) butenes (B; which include iso-butene, 1-butene, trans-2-butene and cis-2-butene isomers), iv) aromatics (BTX; benzene, toluene and xylenes), v) C_5-C_{10} aliphatics (C_5^+), vi) C_2-C_4 paraffins (Pa; ethane, propane, i-butane and n-butane), vii) methane, viii) carbon monoxide, ix) dimethyl ether (D), x) methanol (M), and xi) water (W).

3. Results and discussion

3.1. Coke deposition and deactivation

The TPO profile corresponding to the combustion of the coke deposited on the catalyst under certain conditions is shown in Figure 1 as an example (the TPO profiles corresponding to other reaction temperatures are shown in Figure S1 of the supplementary information). Moreover, the profiles of three fractions of coke determined by deconvolution of the TPO curve are also depicted, with peak maximums at 673 K (coke C1), 743 K (coke C2) and 823 K (C3). According to the literature about the composition of coke deposited on SAPO-34 [39-42] and HZSM-5 zeolite catalysts [18,19,43,44], these peaks can be associated to three fractions of coke with different nature and location in the porous structure of the catalyst particle. Thus, coke C1 (maximum at 673 K) can be attributed to a low developed coke with high H/C ratio and located in the mesopores of the matrix of the catalyst particle. The other two fractions of coke, C2 and C3, are referred to coke structures located in the crystalline channels of the zeolite, but their different combustion temperatures suggest a different composition. Coke C2 (maximum at 743 K) is presumably composed of oxygenated species, formed by secondary reactions between methoxy ions and reaction intermediates [18]. On the other hand, coke C3 (fraction that burns with more difficulty, maximum at 823 K),

corresponds to more condensed species, which are presumably the polymethylbenzenes intermediates of the reaction retained in the crystalline channels [40].

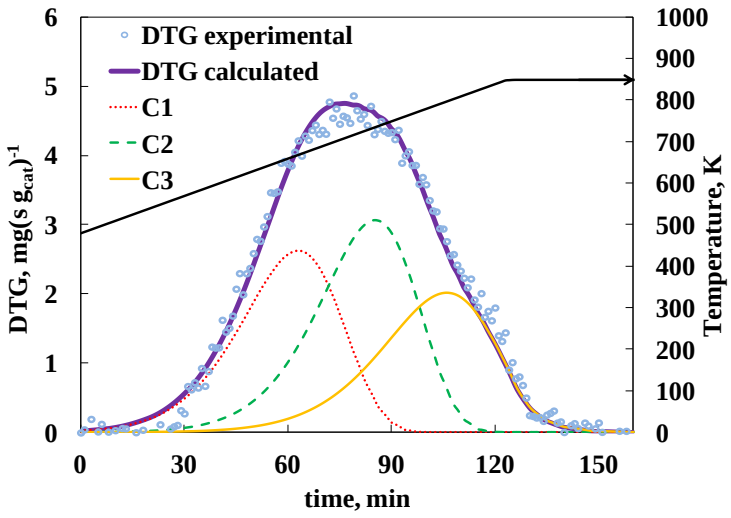

Figure 1. TPO curve deconvolution and identification of three fractions of coke (C1, C2, C3) deposited on the deactivated catalyst. Reaction conditions: temperature, 623 K; space time, 1.5 g_{cat} h mol_C^{-1}; feed, pure DME; time on stream, 18 h.

As a consequence of the coke deposition, DME conversion decreases with time on stream. As an example, Figure 2a illustrates this evolution for three values of space time. The conversion has been defined as:

$$X = \frac{\sum F_i}{F_0} 100 \qquad (1)$$

where F_i and F_0 are the molar flow rates of the *i* compound in the product stream and DME fed, respectively, in C units. The formed water and oxygenates (methanol or DME in thermodynamic equilibrium) have not been considered in the $\sum F_i$ term.

TPO profiles of the catalysts deactivated under the operating conditions of Figure 2a, along with the total coke content in each case are shown in Figure 2b. It is observed that the deposited coke content decreases when increasing the space time. These results are related to the lower DME concentration in the reaction medium when increasing the space time (due to the higher conversion, Figure 2a) and to the higher water concentration in the medium. It is well established that in the methanol conversion, oxygenates in the reaction medium (methanol and DME) are the major responsibles for the coke formation, and water attenuates the coke formation, because it avoids the adsorption and condensation of oxygenates on the acid sites [32-36]. These hypotheses about the effects of the concentration of DME and water on the coke deposition are ascertained in the succeeding sections with the kinetic equation of deactivation.

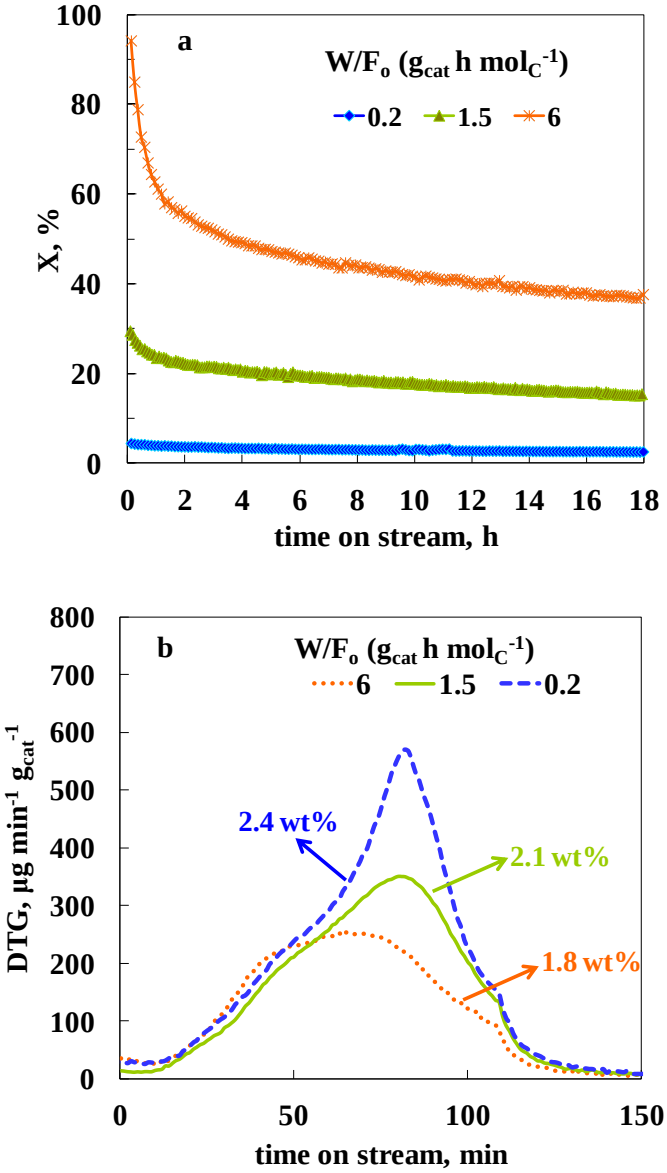

Figure 2. Evolution with the time on stream of DME conversion (a) and TPO curves of the corresponding deactivated catalysts (b). Reaction conditions: feed, pure DME; temperature, 623 K.

The deconvolution of the TPO profiles has been performed by fitting the experimental results to a combustion kinetic of first order for both coke content in the catalyst and oxygen concentration:

$$-\frac{dC_{C_i}}{dt} = k_{Ci} C_{C_i} P_{O_2} = k^*_{Ci} \exp\left[-\frac{E_{Ci}}{R}\left(\frac{1}{T}-\frac{1}{T^*}\right)\right] C_{C_i} P_{O_2} \quad (2)$$

where T^* is the reference temperature (773 K) and $k_{Ci}{}^*$ is the apparent kinetic constant at the reference temperature and C_{Ci} is the content of each *i* fraction of coke.

The Eq. (2) is solved with the initial condition:

$$\text{For} \quad t = 0: \qquad C_{Ci} = f_{Ci}\, C_C \quad (3)$$

where f_{Ci} is the *i* coke fraction and C_C is the total coke content.

The method used for the calculation of the kinetic parameters, that is, the values of the activation energies, E_{Ci}, and the apparent pre-exponential factors, $k_{Ci}{}^*$, has consisted in fitting the results of the deconvolution of the TPO profiles to the Eq. (2), by minimizing the following objective function (using a program written in MATLAB):

$$OF_1 = \frac{\sum_{j=1}^{n}\left[\left(\sum_{i}^{n}\frac{dC_{C_i}}{dt}\right)_{calculated} - \left(\frac{dC_C}{dt}\right)_{experimental}\right]^2}{n \cdot C_C} \quad (4)$$

The results of the total coke contents and the kinetic parameters of coke combustion and temperatures of the deconvoluted peaks for the catalysts deactivated at different reaction temperatures are listed in Table 1. Such results evidence that increasing reaction temperature, both the total coke content and C1 coke fraction decrease, while C2 and C3 fractions increase. This result is consistent with the attenuation of the coke formation when increasing DME conversion and when increasing the concentration of water in the reaction medium [25,26]. The decrease in the total coke content by increasing the space time (Figure 2b) and / or temperature (Table 1) can be explained by the following two causes: i) an increase in the concentration of water in the reaction medium, and ii) a decrease in the concentration of oxygenates (DME and methanol in equilibrium) in the reaction medium. A high concentration of water has the positive effect of sweeping the

coke precursors present in the matrix towards the exterior of the catalyst particle, and consequently the C1 fraction (presumably located in the matrix of γ-Al_2O_3) decreases, which reduces the blockage of the mouths of the micropores and consequently attenuates the loss of the catalyst activity. This effect of the increase in the water content is evident for the C1 coke fraction (coke in the matrix). However, with increasing reaction temperature the contents of the other fractions of coke (C2 and C3) located inside the micropores of the zeolite and related to the oxygenated and aromatic coke, respectively increase. The explanation lies in the fact that increasing reaction temperature, the rates of the oxygenate and polymethylbenzene condensation reactions increase, leading to the formation of coke C2 and C3 fractions. These condensation reactions are catalyzed by the acid sites of the catalyst and their advances are also dependent on the concentration of the reaction medium.

On the other hand, the results in Table 1 support the aforementioned hypothesis of the coke origin and location. The results are consistent with the prior assignment of the TPO peaks to coke fractions of different nature and location. Thus it is observed that the apparent kinetic constants of combustion at the reference temperature have the following order: C1 > C2 > C3, with a remarkable difference between values, indicating an increasing order of combustion difficulty. In the same way, the order of the apparent combustion energy values (reverse to the ease of combustion) is: C1 < C2 < C3.

Table 1. Total coke content (C_C), fraction of each type of coke (f_{Ci}) and kinetic parameters of combustion. Reaction conditions: feed, pure DME; space-time, 1.5 g_{cat} h mol_C^{-1}; time on stream, 18 h.

Temperature, K	**598**	**623**	**648**	**673**
C_C, wt%	2.02	1.93	1.76	1.55
f_{C1} (± 5.90x10^{-3})	0.348	0.330	0.314	0.258
f_{C2} (± 9.64x10^{-3})	0.355	0.363	0.366	0.415
f_{C3} (± 7.78x10^{-3})	0.297	0.307	0.320	0.327
k_{C1}^*, atm^{-1} h^{-1}	148.0 (± 1.5)			
k_{C2}^*, atm^{-1} h^{-1}	46.5 (± 0.4)			
k_{C3}^*, atm^{-1} h^{-1}	10.0 (± 4.6)			
E_{C1}, kJ mol^{-1}	81.6 (± 0.8)			
E_{C2}, kJ mol^{-1}	110.1 (± 0.3)			
E_{C3}, kJ mol^{-1}	115.6 (± 1.0)			
OF_1	4.1x10^{-3}	3.9x10^{-3}	3.2x10^{-3}	8x10^{-3}

3.2. Reaction scheme and kinetic model at zero time on stream

A kinetic model of 11 lumps, which quantifies the product distribution at zero time on stream under the reaction condition ranges studied in this work, has been proposed in a previous work [26]. Figure 3 shows the reaction steps considered in this model. The reaction rate of each *i* lump at zero time on stream has been established considering all the reaction steps in which it is involved:

$$(r_i)_0 = \sum^{j} (\upsilon_i)_j (r_j)_0 \qquad (5)$$

where $(\upsilon_i)_j$ is the stoichiometric coefficient of each *i* lump in the *j* reaction step of the kinetic scheme [26], and $(r_j)_0$ is the reaction rate of the *j* reaction step at zero time on stream.

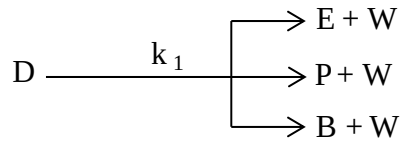

$(r_1)_0 = k_1 p_D \theta$ (6)

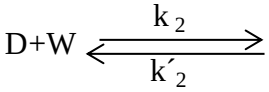

$(r_2)_0 = k_2 [p_D p_W - (p_M^2/K_2)]\theta$ (7)

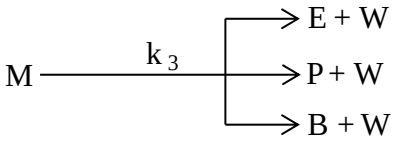

$(r_3)_0 = k_3 p_M \theta$ (8)

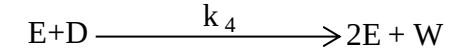

$(r_4)_0 = k_4 p_D p_E \theta$ (9)

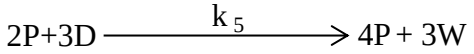

$(r_5)_0 = k_5 p_D p_P \theta$ (10)

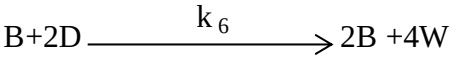

$(r_6)_0 = k_6 p_D p_B \theta$ (11)

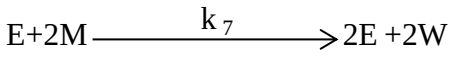

$(r_7)_0 = k_7 p_M p_E \theta$ (12)

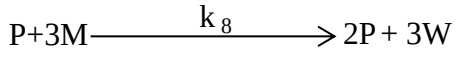

$(r_8)_0 = k_8 p_M p_P \theta$ (13)

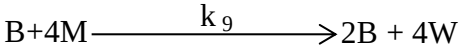

$(r_9)_0 = k_9 p_M p_B \theta$ (14)

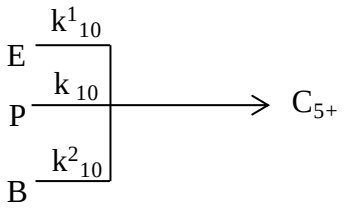

$(r^1_{10})_0 = k^1_{10} p_E \theta = f_1 k_{10} p_E \theta$ (15)

$(r_{10})_0 = k_{10} p_P \theta$ (16)

$(r^2_{10})_0 = k^2_{10} p_B \theta = f_2 k_{10} p_B \theta$ (17)

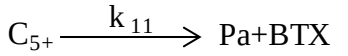

$(r_{11})_0 = k_{11} p_{C5+} \theta$ (18)

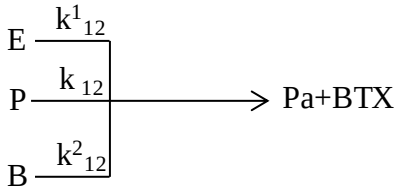

$(r^1_{12})_0 = k^1_{12} p_E \theta = f_1 k_{12} p_E \theta$ (19)

$(r_{12})_0 = k_{12} p_P \theta$ (20)

$(r^2_{12})_0 = k^2_{12} p_B \theta = f_2 k_{12} p_B \theta$ (21)

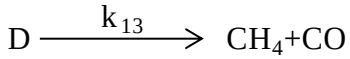

$(r_{13})_0 = k_{13} p_D$ (22)

Figure 3. Steps of DME conversion and reaction rate equations at zero time on stream.

The expressions for the reaction rates ($(r_j)_0$ in Eq. (5)) are also shown in Figure 3 (Eqs. (6-22)) assuming the reaction steps to be elementary and using partial pressures, p_i, to quantify the concentration of each *i* lump. The term θ in the Eqs. (6-21), quantifies the attenuation of the reaction rate of each step by the adsorption of methanol and water on the acid sites:

$$\theta = \frac{1}{1 + K_a\left(p_M + p_W\right)} \tag{23}$$

where K_a is a constant that quantifies the adsorption of both (methanol + water).

The equilibrium constant of step 2 (Eq. (7)) in the scheme in Figure 3 has been estimated using the reverse expression of that established in the literature for methanol dehydration [31]:

$$K_2 = \exp\left(-9.76 + 3200/T + 1.07\ \mathrm{Ln}T - 6.6\ 10^{-4}\ T + 4.9\ 10^{-8}\ T^2 + 6500/T^2\right) \tag{24}$$

The kinetic parameters of the model at zero time on stream [26] have been summarized in Table 2. These parameters have been used in the present work to establish the deactivation kinetic equation and thus, the complete kinetic model.

Table 2. Parameters of the kinetic model at zero time on stream.

Parameter	**k_j^* (at 623 K)**	**E_j (kJ mol^{-1})**
k_1 ($mol_C\ g_{cat}^{-1}\ h^{-1}\ atm^{-1}$)	$(4.99 \pm 0.01)x10^{-2}$	$(4.15 \pm 0.03)x10^{1}$
k_2 ($mol_C\ g_{cat}^{-1}\ h^{-1}\ atm^{-2}$)	$(7.88 \pm 0.50)x10^{1}$	$(1.19 \pm 0.07)x10^{1}$
k_3 ($mol_C\ g_{cat}^{-1}\ h^{-1}\ atm^{-1}$)	$(2.42 \pm 0.15)x10^{-3}$	$(3.38 \pm 0.02)x10^{1}$
k_4 ($mol_C\ g_{cat}^{-1}\ h^{-1}\ atm^{-2}$)	$(2.48 \pm 0.34)x10^{-1}$	$(1.72 \pm 0.02)x10^{1}$
k_5 ($mol_C\ g_{cat}^{-1}\ h^{-1}\ atm^{-2}$)	2.54 ± 0.01	$(2.57 \pm 0.03)x10^{1}$
k_6 ($mol_C\ g_{cat}^{-1}\ h^{-1}\ atm^{-2}$)	$(1.44 \pm 0.88)x10^{-1}$	9.77 ± 0.71
k_7 ($mol_C\ g_{cat}^{-1}\ h^{-1}\ atm^{-2}$)	$(3.02 \pm 0.05)x10^{1}$	$(1.63 \pm 0.01)x10^{1}$
k_8 ($mol_C\ g_{cat}^{-1}\ h^{-1}\ atm^{-2}$)	2.63 ± 0.09	$(1.69 \pm 0.03)x10^{1}$
k_9 ($mol_C\ g_{cat}^{-1}\ h^{-1}\ atm^{-2}$)	$(4.24 \pm 1.14)x10^{-1}$	$(6.90 \pm 0.03)x10^{1}$
k_{10} ($mol_C\ g_{cat}^{-1}\ h^{-1}\ atm^{-1}$)	1.03 ± 0.01	$(2.12 \pm 0.01)x10^{1}$
k_{11} ($mol_C\ g_{cat}^{-1}\ h^{-1}\ atm^{-1}$)	$(1.16 \pm 2.54)x10^{-2}$	$(6.01 \pm 1.35)x10^{-1}$
k_{12} ($mol_C\ g_{cat}^{-1}\ h^{-1}\ atm^{-1}$)	$(3.10 \pm 0.02)x10^{-1}$	$(2.05 \pm 0.01)x10^{1}$
k_{13} ($mol_C\ g_{cat}^{-1}\ h^{-1}\ atm^{-1}$)	$(5.63 \pm 1.10)x10^{-4}$	$(3.37 \pm 0.04)x10^{1}$
K_a^* (atm^{-1})	$(1.27 \pm 0.01)x10^{1}$	
ΔH_a (kJ mol^{-1})	$(1.98 \pm 0.5)x10^{-1}$	
f_1	1.78 ± 0.02	
f_2	$(6.92 \pm 0.19)x10^{-1}$	

3.2.1. Proposed deactivation kinetic equation and calculation methodology

A quasi nonselective deactivation has been considered to determine the lessening of the reaction rates of the steps in Figure 3, in which a common activity has been assumed for all the hydrocarbon formation rates (Eqs. (6) and (8-21) corresponding to steps 1 and 3-12 in Figure 3). However, the experimental results suggest a negligible deactivation of steps 2 (DME hydrolysis) and 13 (CH_4 formation) [25], and therefore, the activity has been considered to be constant and equal to the unity in these steps. This consideration is also based on the well known weak acidity necessary for hydrolyzing DME and the thermal cracking mechanism of CH_4 formation (without any effect on catalyst activity).

The aforementioned results of product yields evolution with time on stream [25] and coke deposition (Table 1) highlight the influence of other factors on the catalyst deactivation, which have to be considered in the kinetic equation. Therefore, in the conversion of DME, as occurs in the methanol to hydrocarbons conversion [31,34-36], catalyst deactivation increases upon increasing oxygenates concentration (methanol and DME) in the reaction medium, and decreases when increasing the concentration of water [25]. Consequently, the following general expression has been established for the deactivation kinetic equation (Parent model, *A*):

$$-\frac{da}{dt} = k_d p_D a^d \theta_d \qquad (25)$$

In Eq. (25) activity (a) is defined as the ratio between the reaction rates of step *j* at *t* time and at zero time on stream:

$$a = \frac{r_j}{(r_j)_0} \qquad \text{(for } j\text{= 1 and 3-12 in Figure 3)} \qquad (26)$$

Term θ_d in Eq. (25) quantifies the catalyst deactivation attenuation by the adsorption of water on the acid sites of the catalyst using the following expression that resulted adequate for the deactivation kinetics of methanol conversion [31]:

$$\theta_d = \frac{1}{1 + K_{W,d} p_W} \tag{27}$$

where the term $K_{w,d}$ is related to the equilibrium constant of the adsorption of water on the acid sites. For the calculation, the equilibrium constants have been reparameterized. Thus for $K_{w,d}$:

$$K_{W,d} = K^*_{W,d} \exp\left[- \frac{\Delta H_{W,d}}{R} \left(\frac{1}{T} - \frac{1}{T^*} \right) \right] \tag{28}$$

The activity term (a) has been included in the formation rates of each compound in steps 1 and 3-12 of the kinetic scheme in Figure 3 in order to consider the deactivation in the kinetic model of the process:

$$r_i = \sum^{j} (\upsilon_i)_j (r_j)_0 a \tag{29}$$

The methodology used for data analysis and for the calculation of the kinetic parameters has been described in previous papers for other catalytic processes of complex reaction schemes and considers the “past history” of the catalyst in each longitudinal position of the fixed-bed reactor [31,34-36,45]. On the other hand, the general criteria used are consistent with those established by Toch et al. [46] for the kinetic modeling of catalytic processes without considering deactivation. The kinetic parameters of best fit have been calculated by multivariable nonlinear regression between the experimental results and the corresponding values calculated integrating the kinetic model along with the deactivation kinetic equation. The optimization has been carried out by minimizing the following objective function:

$$OF_2 = \sum_{i=1}^{n_l} \omega_i \varphi_i = \sum_{i=1}^{n_l} \omega_i \sum_{j=1}^{p} R_j \left(Y_{i,j}^{*} - Y_{i,j} \right)^2 \quad (30)$$

where: ω_i is the weight factor for each lump *i* of the kinetic scheme; φ_i is the sum of squares for the lack of fit for each lump (including the runs repeated under the same operating conditions, R_j); n_l is the number of lumps in the kinetic scheme; p is the total number of experimental conditions (including repetitions or not); $Y_{i,j}^{*}$ is the experimental value of concentration (molar fraction, referred to the organic compounds in the reaction medium, in C units) of each lump *i* for the *j* experimental condition; and $Y_{i,j}$ is the corresponding value calculated by integrating the mass balance for the lump *i*, considering deactivation.

Ideal flow (plug flow) and isothermal regime have been assumed in the catalytic bed, since the temperature differences at different radial and longitudinal positions are lower than 2 K. Consequently, the evolution of the composition of each lump *i* in the reactor has been determined with the corresponding mass conservation equation:

$$r_i = \frac{dY_i}{d\left(W/F_0\right)} \quad (31)$$

where W is the catalyst mass, in g.

The deactivation kinetic constants have been expressed using the Arrhenius reparameterized equation, so that deactivation kinetic constants at reference temperature (623 K) and the corresponding activation energies are the parameters to be optimized.

A MATLAB program based on fourth-order finite-difference approximation has been used for the integration of the kinetic equations and for the multivariable nonlinear regression, which allows the kinetic parameter calculation. The optimization has been carried out by minimizing the objective function (Eq. (30)) using successive routines, as described in detail elsewhere [26].

The significance test of the proposed model has been carried out based on the analysis of variance [45,47,48]. The variances for the lack of fit of the model, s_a^2, and for the pure experimental error (calculated from the repeated runs), s_e^2, are compared to assess the model significance. Thus, when the ratio between these variances is below critical, the lack of fit is not significant and the model does not require further improvement. The F-test statistics are calculated according to the following expression:

$$F_{a-e} = \frac{s_a^2}{s_e^2} < F_{1-\alpha}(\upsilon_a, \upsilon_e) \tag{32}$$

In Eq. (32) the critical value of the Fischer distribution function, $F_{1-\alpha}$ (ν_a, ν_e), is a function of the degrees of freedom for the compared variances (a, e) and of the percentage of confidence sought for the comparison, 100(1-α). This value is calculated using the function *finv(1-α,v_a,v_e)* of MATLAB. The variances s_a^2 and s_e^2 are calculated as the ratio of the corresponding values of the sum of squares and degrees of freedom.

3.2.2. Kinetic parameters and fitting of the model to the experimental results

The kinetic results at zero time on stream (Table 2) obtained in a previous work [26] have been used for the calculation and therefore, the parameters to be calculated are: the deactivation kinetic constant at reference temperature, k_d^*; the corresponding activation energy, E_d; deactivation order, d; apparent equilibrium constant of water adsorption at reference temperature, $K_{W,d}^*$; and its respective term of apparent adsorption heat, $\Delta H_{w,d}$.

The deactivation kinetic parameters of the model of best fit and the corresponding confidence intervals (95 %) have been listed in Table 3. Besides, the indices for the fitting quality of the model to the experimental results and the value of the objective function (Eq. (30)) are shown in Table 4. Such data reveals that the model satisfies the

required significance test, since the error for the lack of fit of the model is comparable to the pure experimental error.

Table 3. Kinetic parameters of best fit of the proposed deactivation equation (Eq. 25).

k^{*}_{d1}, h atm^{-1}	$(7.88 \pm 0.42)x10^{-1}$
E_{d1}, kJ mol^{-1}	$(1.64 \pm 0.28)x10^{1}$
d	(4.87 ± 0.03)
$K^{*}_{W,d}$, h atm^{-1}	$(3.01 \pm 0.54)x10^{-2}$
$\Delta H_{W,d}$, kJ mol^{-1}	$(4.87 \pm 0.22)x10^{1}$

Table 4. Objective function and variance analysis for the deactivation equation.

OF_2	$1.36x10^{-1}$
s_e^2	$3.15x10^{-4}$
s_a^2	$3.5x10^{-4}$
s_e^2/s_a^2	1.11
$F_{1-\alpha}(\upsilon_a, \upsilon_e)$	1.24
Significance test	Valid

It should be noted that the high deactivation order (d = 4.87) indicates that the activity of the catalyst decreases with time on stream tending to a pseudo-equilibrium state. This

is a well known trend in the reactions carried out over HZSM-5 zeolite catalysts, in which the rate of coke deposition on the crystalline channels of the zeolite equals the coke entrainment rate by the reaction medium. This phenomenon is favored by the moderate molecular weight of the coke species and by the structure of the HZSM-5 zeolite without boxes in the intersections between channels [49]. It should be noted that since the deactivation results tend to constant conversion values, a kinetic model considering residual activity could be interesting. These models are useful in catalytic processes under the following circumstances [50] i) catalysts with active sites of different strength; ii) reversible formation of coke (as in the reaction studied in this work), and iii) simultaneous generation and disappearance of the active sites. These equations, offer a better fit of the deactivation results than the equations in which a residual activity is not considered [51,52]. However, determining the residual activity at certain reaction conditions as an adjustable parameter, has a high level of empiricism and also requires experiments with high values of time on stream. On the other hand, in order to avoid the aforementioned empiricism, the goal of the equations that consider a residual activity is to justify the values of this activity with a better comprehension of the reaction mechanism.

On the other hand, the study on the heterogeneity of the coke and its distribution between the matrix and the crystalline channels of the zeolite is of great interest for future works addressed towards minimizing deactivation by tailoring catalyst properties (porous structure and acid strength) aiming to improve the value of the pseudo-stable activity of the catalyst.

The goodness of fit is shown in Figures 4-7. These Figures compare the evolution with time on stream (up to 18 h) of the experimental results (points) and those calculated with the kinetic model (lines) of the molar fractions of the compounds in the reaction

medium at the reactor outlet, referred to organic compounds. The results correspond to pure DME feeds and different temperatures (598, 623, 648 and 673 K, in Figures 4, 5, 6 and 7, respectively).

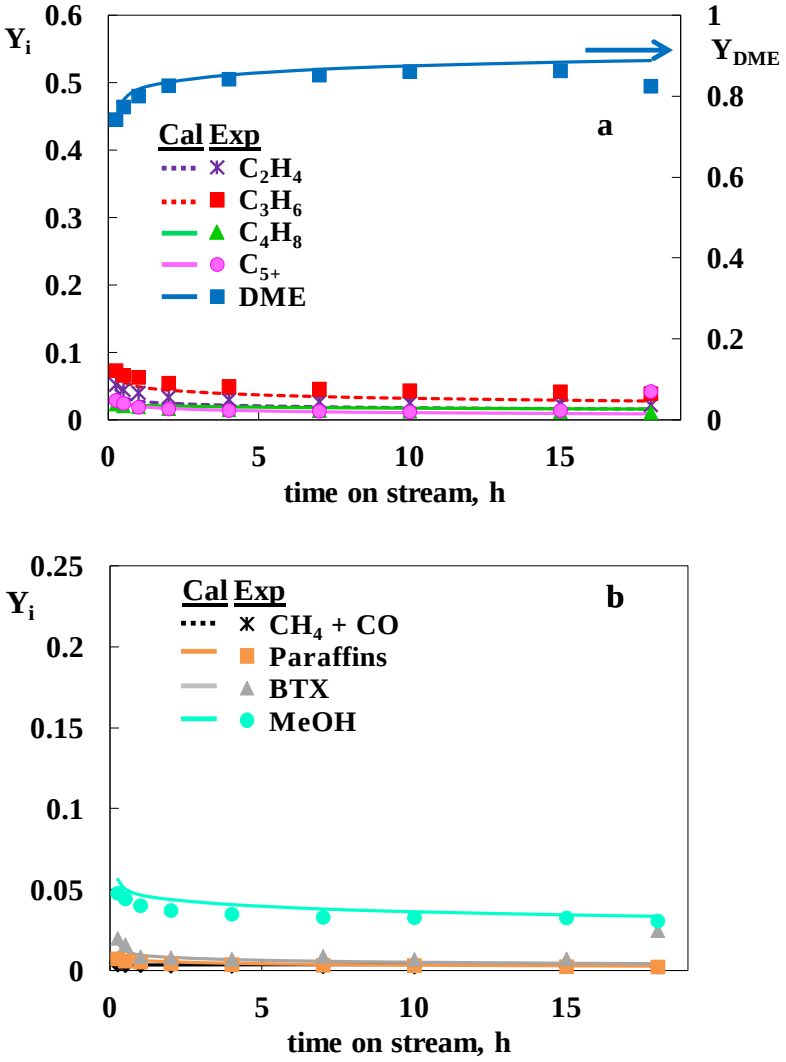

Figure 4. Comparison of the evolution with the time on stream of the experimental values (points) of the molar fractions with those calculated using the deactivation equation (A model) (lines) for the major compounds (a) and the minor compounds (b). Reaction conditions: feed, pure DME; temperature, 598 K; space time, 3 g_{cat} h mol_C^{-1}.

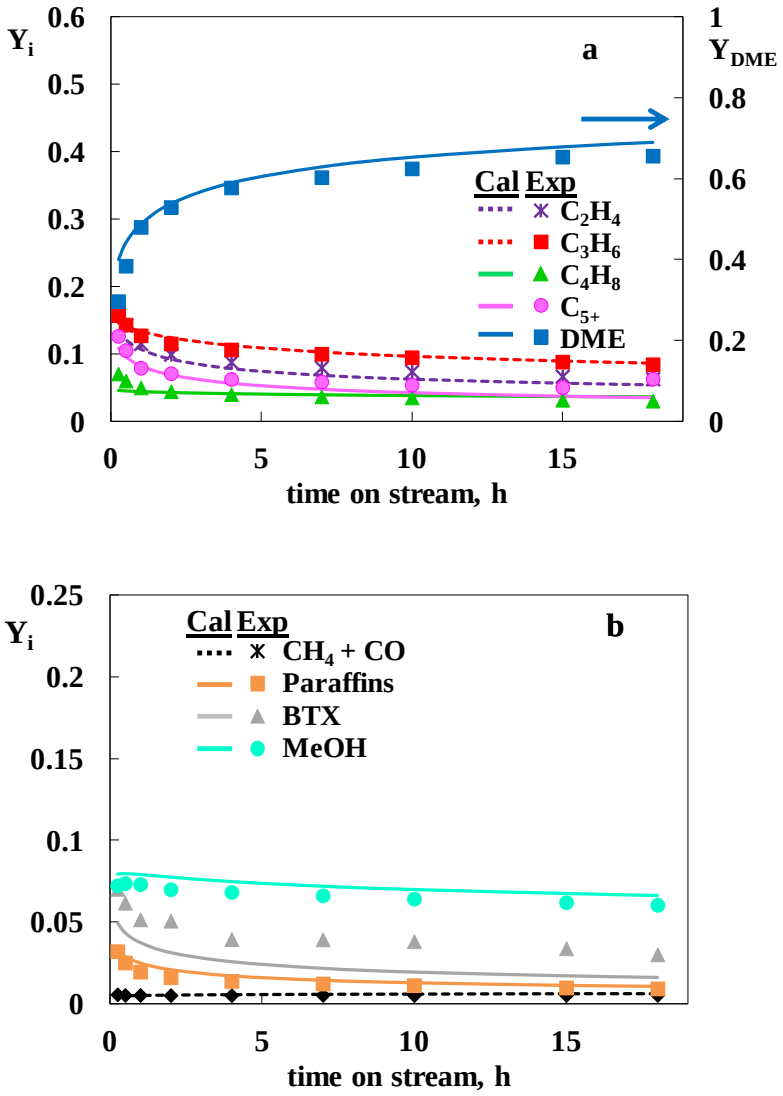

Figure 5. Comparison of the evolution with the time on stream of the experimental values (points) of the molar fractions with those calculated using the deactivation equation (A model) (lines) for the major compounds (a) and the minor compounds (b). Reaction conditions: feed, pure DME; temperature, 623 K; space time, 3 g_{cat} h mol_C^{-1}.

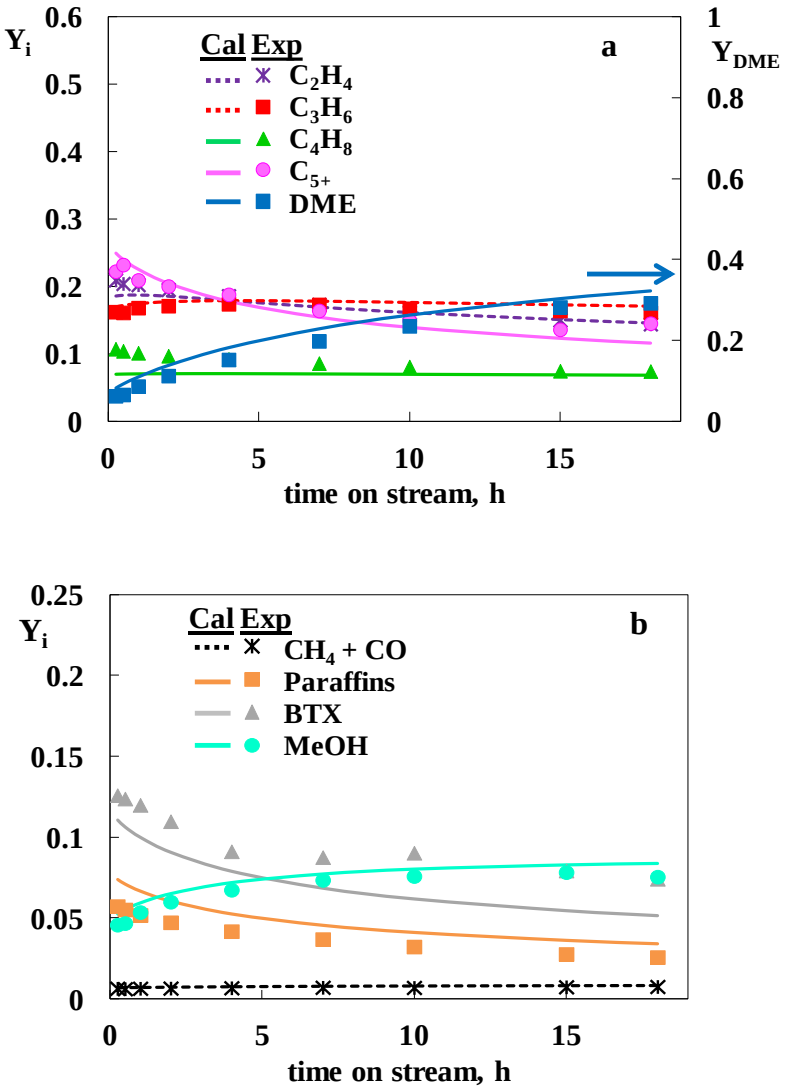

Figure 6. Comparison of the evolution with the time on stream of the experimental values (points) of the molar fractions with those calculated using the deactivation equation (A model) (lines) for the major compounds (a) and the minor compounds (b). Reaction conditions: feed, pure DME; temperature, 648 K; space time, 3 g_{cat} h mol_C^{-1}.

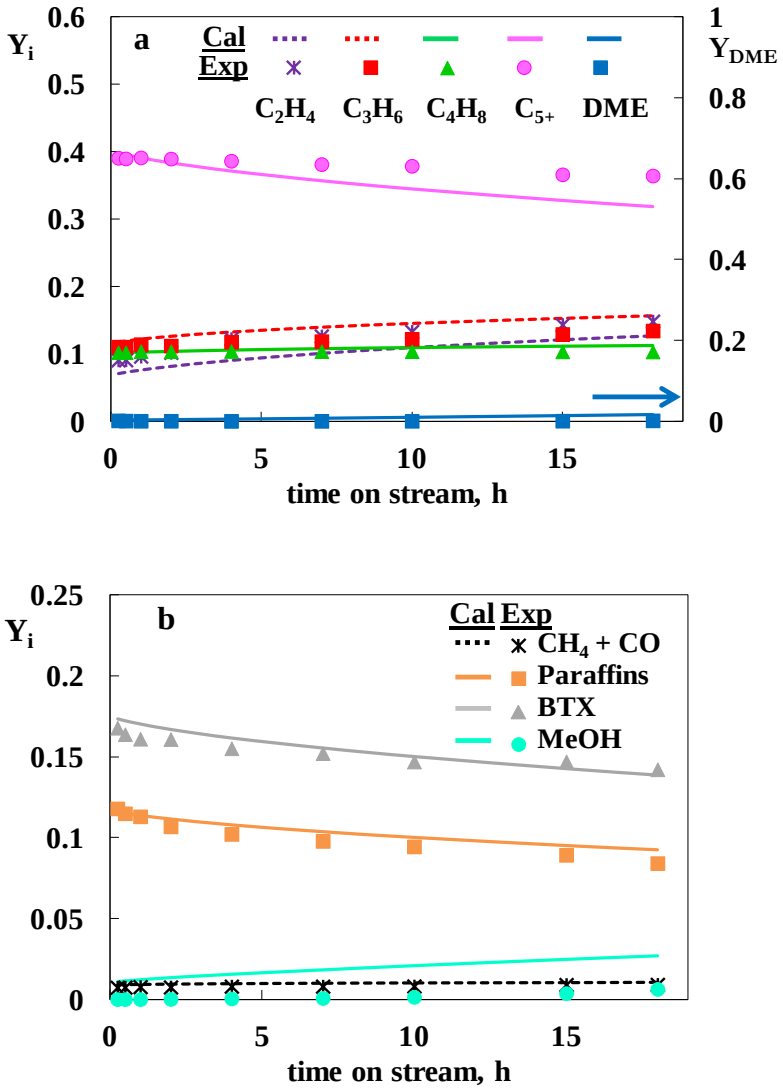

Figure 7. Comparison of the evolution with the time on stream of the experimental values (points) of the molar fractions with those calculated using the deactivation equation (A model) (lines) for the major compounds (a) and the minor compounds (b). Reaction conditions: feed, pure DME; temperature, 673 K; space time, 3 g_{cat} h mol_C^{-1}.

In addition, the proposed kinetic model also fits satisfactorily the evolution with time on stream of product distribution when feeding DME diluted with He, water and methanol, as depicted in Figures 8, 9 and 10, respectively. The model is suitable for its use in further simulation studies aimed on the one hand to quantify the optimal content of He

and water in the feed stream in order to attenuate deactivation, and on the other hand to the recirculation of the methanol formed as by-product.

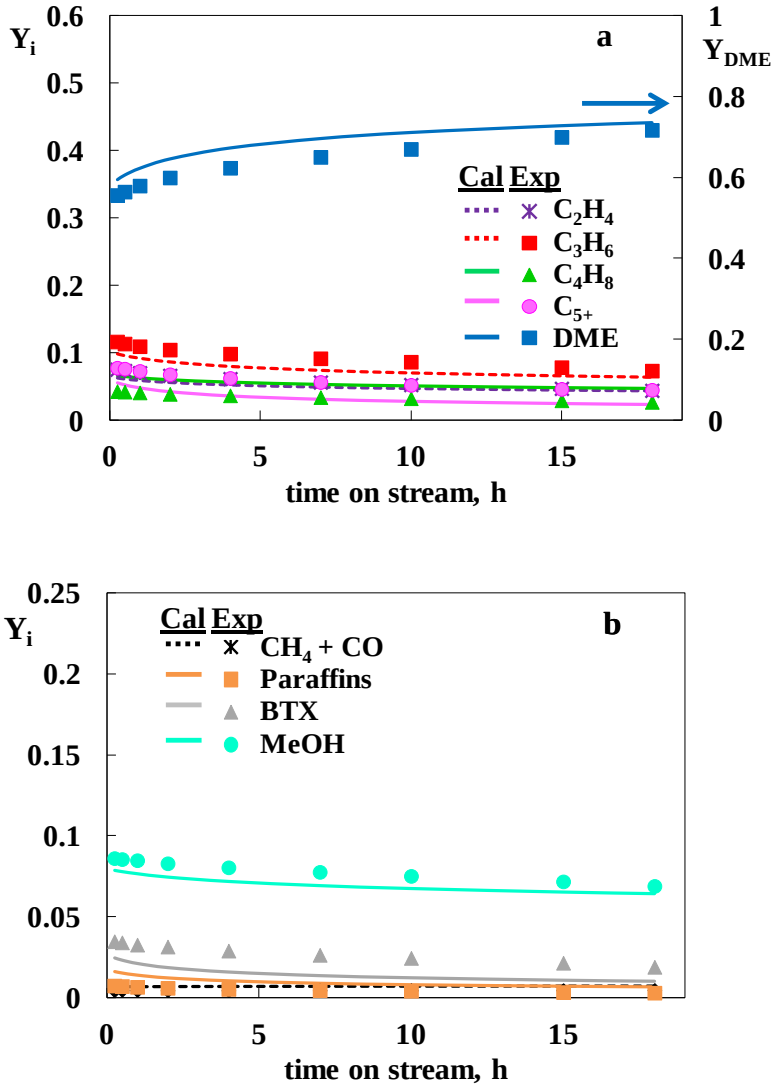

Figure 8. Comparison of the evolution with the time on stream of the experimental values (points) of the molar fractions with those calculated using the deactivation equation (A model) (lines) for the major compounds (a) and the minor compounds (b). Reaction conditions: feed, DME diluted with 50 % of He; temperature, 648 K; space time, 1 g_{cat} h mol_C^{-1}.

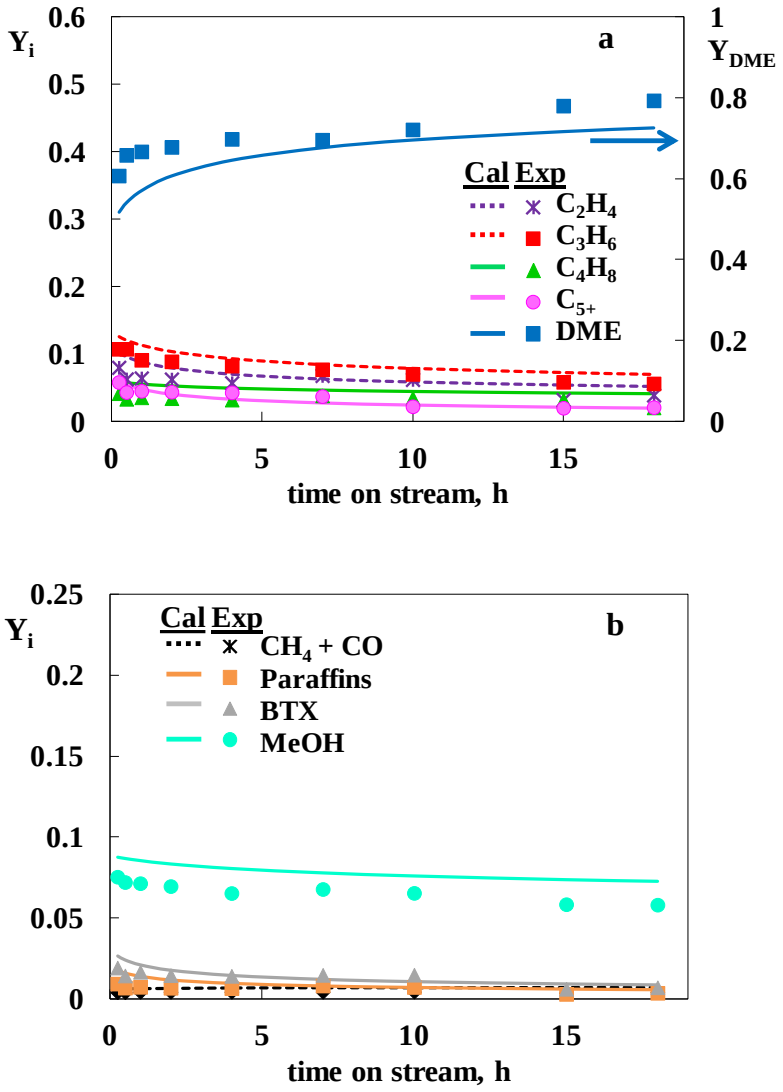

Figure 9. Comparison of the evolution with the time on stream of the experimental values (points) of the molar fractions with those calculated using the deactivation equation (A model) (lines) for the major compounds (a) and the minor compounds (b). Reaction conditions: feed, DME diluted with 5 % of H_2O; temperature, 648 K; space time, 1 g_{cat} h mol_C^{-1}.

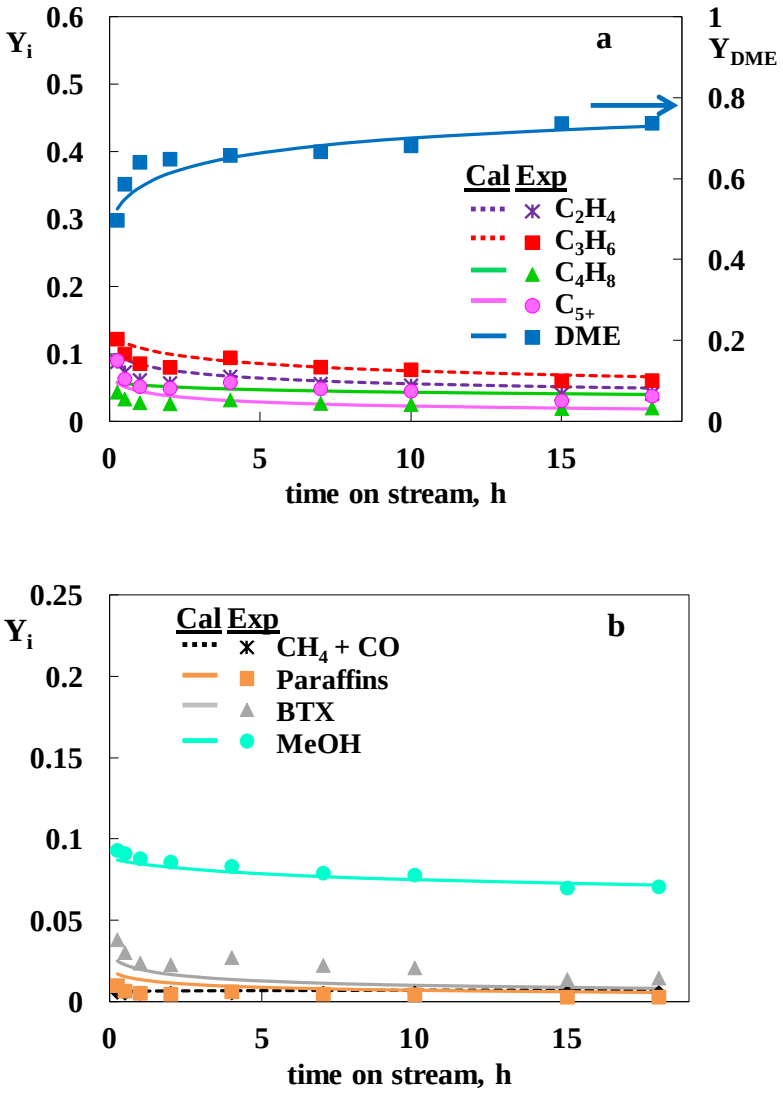

Figure 10. Comparison of the evolution with the time on stream of the experimental values (points) of the molar fractions with those calculated using the deactivation equation (A model) (lines) for the major compounds (a) and the minor compounds (b). Reaction conditions: feed, DME diluted with 5 % of methanol; temperature, 648 K; space time, 1 g_{cat} h mol_C^{-1}.

Overall, a good fitting of the experimental results is obtained for the different conditions shown and in the whole studied operating range.

3.2.3. Other deactivation kinetic equations

Table 5 summarizes other studied deactivation kinetic equations of different complexity, whose fitting to the experimental results has also been studied.

Table 5. Other deactivation equations studied.

Model	Coke precursors	Deactivation equation
B	All components	$-\frac{da}{dt} = k_{d1} P\, a^{d} \theta_{d}$ (33)
C	Oxygenates (MeOH and DME)	$-\frac{da}{dt} = (k_{d1} p_{M} + k_{d2} p_{D}) a^{d} \theta_{d}$ (34)
D	Olefins and hydrocarbons (O + C_{5+})	$-\frac{da}{dt} = k_{d1} (p_{O} + p_{C5+}) a^{d} \theta_{d}$ (35)
E	Paraffins and aromatics	$-\frac{da}{dt} = k_{d1} (p_{Pa} + p_{BTX}) a^{d} \theta_{d}$ (36)
F	Oxygenates, olefins and hydrocarbons	$-\frac{da}{dt} = [k_{d1} (p_{M} + p_{D}) + k_{d2} (p_{O} + p_{C5+})] a^{d} \theta_{d}$ (37)

In model *B* (Eq. (33)), deactivation has been considered to be independent of the progress of the reaction, since all the carbonaceous components in the reaction medium have the same capacity for coke formation. In model *C* (Eq. (34)) oxygenates (methanol and DME) are considered to be the unique coke precursors and thus that coke formation occurs in parallel with the formation of the reaction products. Models *D* and *E* (Eqs. (35) and (36), respectively) consider deactivation in series, with the products as coke precursors. These precursors are the light olefins and heavy compounds in model *D*, and light paraffins and aromatics in model *E*. Model *F* (Eq. (37)) considers deactivation to

take place in series-parallel with the reaction scheme, considering the oxygenates and the major compounds (light olefins and heavy aliphatics) as coke precursors, with different contributions quantified by k_{d1} and k_{d2} constants. The kinetic parameters and the objective function (OF_2) obtained with the new kinetic models are set out in Table 6.

Table 6. Kinetic parameters of best fit and objective function for the deactivation Eqs. (33) - (37).

	Models				
	B	**C**	**D**	**E**	**F**
k_{d1}, h atm^{-1}	$1.46x10^{-1}$	$6.05x10^{-1}$	2.42	$5.61x10^{1}$	$4.25x10^{-1}$
k_{d2}, h atm^{-1}	-	$6.01x10^{-1}$	-	-	$5.46x10^{-2}$
E_{d1}, kJ mol^{-1}	$3.40x10^{1}$	7.50	$4.63x10^{1}$	$4.65x10^{1}$	1.25
E_{d2}, kJ mol^{-1}	-	7.44	-	-	4.99
k_{dads}, h atm^{-1}	$8.22x10^{-1}$	$2.34x10^{-2}$	$3.84x10^{-2}$	$4.55x10^{-1}$	$3.22x10^{-2}$
E_{dads}, kJ mol^{-1}	$5.42x10^{-1}$	$3.03x10^{-1}$	$7.56x10^{-1}$	$1.23x10^{-2}$	$5.21x10^{-1}$
d	3.32	5.55	3.83	7.95	5.45
OF_2	$1.70x10^{-1}$	$1.44x10^{-1}$	$1.62x10^{-1}$	$1.80x10^{-1}$	$1.53x10^{-1}$

Regarding the quality of fit of the different studied kinetic models (OF_2 values in Table 4 for parent Model A and in Table 6 for Models B-F), it should be noted that the best fit corresponds to the models in which DME (model A) and oxygenates (DME and methanol) (model C) have been considered as precursors of the coke, responsible of the catalyst deactivation. The small difference between the fitting qualities of both models is attributed to the fact that even if a better fitting of the model A indicates a greater

activity of DME to form coke precursors, the concentrations of DME and methanol are closely related. Thus a higher concentration of DME leads to a higher concentration of methanol, since the thermodynamic equilibrium between both is quickly reached. In addition, the kinetic model at zero time on stream [26] and other previous experimental and kinetic results [34] have shown that DME is more reactive than methanol. Based on studies in literature regarding reaction mechanisms, this higher reactivity is justified by the higher proton affinity of DME and thus the greater ability to form methoxy species [27], and also by the existence of a route additional to the dual cycle mechanism (feature of methanol conversion, with polymethylbencenes and olefins as intermediates) [28]. Consequently, the major responsibility of DME as a coke precursor and therefore, as the main responsible for the deactivation of the catalyst, can be related to the higher formation rate of the methoxy species (presumably the precursors of the formation of the oxygenate components of coke, present in the C2 fraction) and the transformation of these into polymethybenzenes (intermediates in the formation of the condensate coke C3 fraction).

The consideration as precursors of the coke formation of the oxygenates and olefins along with the C_{5+} aliphatic hydrocarbons in the reaction medium (model F) results in a worse fit than those obtained with models A and C. This reinforces the hypothesis that the mechanism of coke formation runs in parallel with the mechanism of the main reaction. This occurs after the adsorption of DME in the active sites, the subsequent generation of intermediates and the condensation of these on the active sites, thus being secondary the role of the not adsorbed olefins and aromatics. This hypothesis of the role of DME as the responsible reactant for the formation of coke, is consistent with the worse fit obtained with other models that do not directly consider the concentration of DME in the kinetic model (models D and E) or consider all the components in the

reaction medium (oxygenates, paraffins, olefins and aromatics) as responsible for the deactivation (Model B).

On the other hand, in order to evaluate the significance of the improvement achieved with a given equation compared with a simpler equation, the analysis of variances should be pefformed. A criterion to asses if model *j* (complex model) is significantly better than model *i* (simpler model) is to evaluate if the following expression is fulfilled [53]:

$$F_{i-j} = \frac{(SSE_i - SSE_j)/SSE_j}{(\upsilon_i - \upsilon_j)/\upsilon_j} > F_{1-\alpha}(\upsilon_i - \upsilon_j, \upsilon_j) \qquad (38)$$

where SSE_i and SSE_j are the sum of squares of each model, $F_{1-\alpha}(\upsilon_i-\upsilon_j, \upsilon_j)$ is the critical value of the Fischer distribution function, and υ_i and υ_j are the degrees of freedom of each model. Table 7 sets out the parameters of the analysis of variance for each model.

Table 7. Parameters for the variance analysis of the deactivation equations.

	Models					
	Parent (A)	**B**	**C**	**D**	**E**	**F**
p	39	39	39	39	39	39
n_l	10	10	10	10	10	10
q	3	3	5	3	3	5
$\upsilon_i = p\ n_l - q$	387	387	385	387	387	385
SSE	$1.36x10^{-1}$	$1.7x10^{-1}$	$1.44x10^{-1}$	$1.62x10^{-1}$	$1.80x10^{-1}$	$1.53x10^{-1}$
s_i^2 (10^4)	3.50	4.40	3.74	4.18	4.65	3.97

Comparing the complexity of the kinetic models studied, the order is as follows: A ≈ *B* ≈ *D* ≈ *E* < C ≈ *F*. Consequently, as the best fit corresponds to the simplest kinetic model (parent model A), the use of the aforementioned significance test is not necessary. Thus, the comparison of more complex models (C and F) with the parent model (A) results in negative values of the F_{i-j} parameter.

4. Conclusions

The TPO analysis of the HZSM-5 zeolite catalyst with high SiO_2/Al_2O_3 ratio, used in the conversion of DME to olefins under different reaction conditions, shows that coke deposition is favored by increasing DME concentration in the reaction medium, and this deposition is attenuated by increasing the concentration of water in the medium. The proposed deactivation kinetic equation considers both effects, as well as the effect of temperature and the remaining activity of the catalyst.

The use of the deactivation kinetic equation together with the kinetic model of 11 lumps established in a previous work for the conversion of DME to light olefins at zero time on stream over the same catalyst, allows for simulating the evolution with time on stream (up to 18 h) of the light olefin concentrations and the fractions of the rest of the products, in a wide operating condition range (temperature, 573-673 K; space time, 0.2-6 g_{cat} h mol_C^{-1}) and for pure DME feeds or diluted with He, water and methanol.

The deactivation kinetic model considers the same deactivation kinetic equation for the majority of the steps of the reaction scheme, being a quasi non-selective model. Deactivation is not considered in the steps of DME hydrolysis (where deactivation is insignificant) and the formation of CH_4 (whose nature is the thermal cracking of

methanol and DME). Furthermore, more complex expressions of the deactivation kinetic equation do not improve the fitting of the results.

Moreover, it has been found that the deposited coke has a heterogeneous nature and is distributed between the matrix and the crystalline channels of the zeolite, what arouses theinterest for minimizing deactivation by tailoring catalyst properties such as porous structure and acid strength.

Acknowledgements

This work was carried out with the financial support of the Ministry of Economy and Competitiveness of the Spanish Government and FEDER funds (CTQ2010-19188 and CTQ2013-46173-R), the Basque Government (Project IT748-13) and the University of the Basque Country (UFI 11/39). Paula Perez-Uriarte is grateful for the Ph.D. grant from the Ministry of Economy and Competitiveness of the Spanish Government (BES-2011-046266).

References

[1] J. Sun, G. Yang, Y. Yoneyama, N. Tsubaki, Catalysis chemistry of dimethyl ether synthesis, ACS Catal. 4 (2014) 3346-3356.

[2] M. Melikoglu, Shale gas: Analysis of its role in the global energy market, Renew. Sust. Energy Rev. 37 (2014) 460-468.

[3] A.T. Aguayo, J. Ereña, D. Mier, J.M. Arandes, M. Olazar, J. Bilbao, Kinetic modelling of dimethyl ether synthesis in a single step on a CuO-ZnO-Al_2O_3/γ-Al_2O_3 catalyst, Ind. Eng. Chem. Res. 46 (2007) 5522-5530.

[4] S. Bhattacharya, K.B. Kabir, K. Hein, Dimethyl ether synthesis from Victorian brown coal through gasification - Current status, and research and development needs, Prog. Energy Combust. Sci. 39 (2013) 577-605.

[5] G.A. Olah, A. Goeppert, G.K.S. Prakash, Chemical recycling of carbon dioxide to methanol and dimethyl ether: From greenhouse gas to renewable, environmentally carbon neutral fuels and synthetic hydrocarbons, J. Organic Chem. 74 (2009) 487-498.

[6] J. Ereña, I. Sierra, A.T. Aguayo, A. Ateka, M. Olazar, J. Bilbao Kinetic modelling of dimethyl ether synthesis from (H_2+CO_2) by considering catalyst deactivation, Chem. Eng. J. 174 (2011) 660-667.

[7] M.H. Zhang, Z.M. Liu, G.D. Lin, H.B Zhang, Pd/CNT-promoted $CuZrO_2$/HZSM-5 hybrid catalysts for direct synthesis of DME from CO_2/H_2, Appl. Catal. A 451 (2013) 28-35.

[8] A. Ateka, I. Sierra, J. Ereña, J. Bilbao, A.T. Aguayo, Performance of CuO–ZnO–ZrO_2 and CuO–ZnO–MnO as metallic functions and SAPO-18 as acid function of

the catalyst for the synthesis of DME co-feeding CO_2, Fuel Process. Technol. 152 (2016) 34-45.

[9] M. Ghavipour, R.M. Behbahani, G.R. Moradi, A. Soleimanimehr, Methanol dehydration over alkali-modified H-ZSM-5: Effect of temperature and water dilution on products distribution, Fuel 113 (2013) 310-317.

[10] M. Bjørgen, S. Svelle, F. Joensen, J. Nerlov, S. Kolboe, F. Bonino, L. Palumbo, S. Bordiga, U. Olsbye, Conversion of methanol to hydrocarbons over zeolite H-ZSM-5: On the origin of the olefinic species, J. Catal. 249 (2007) 195-207.

[11] S. Ilias, A. Bhan, Mechanism of the catalytic conversion of methanol to hydrocarbons, J. Catal. 3 (2013) 18-31.

[12] X. Sun, S. Mueller, Y. Liu, H. Shi, G.L. Haller, M. Sanchez-Sanchez, A.C. Van Veen, J.A. Lercher, On reaction pathways in the conversion of methanol to hydrocarbons on HZSM-5, J. Catal. 317 (2014) 185-197.

[13] C. Wang, J. Xu, G. Qi, Y. Gong, W. Wang, P. Gao, Q. Wang, N. Feng, X. Liu, F. Deng, Methylbenzene hydrocarbon pool in methanol-to-olefins conversion over zeolite H-ZSM-5, J. Catal. 332 (2015) 127-137.

[14] A.T. Aguayo, A.E. Sánchez del Campo, A.G. Gayubo, A.M. Tarrío, J. Bilbao, Deactivation by coke of a catalyst based on a SAPO-34 in the transformation of methanol into olefins, J. Chem. Tech. Biotechnol. 74 (1999) 315-321.

[15] D. Chen, K. Moljord, T. Fuglerud, A. Holmen, The effect of crystal size of SAPO-34 on the selectivity and deactivation of the MTO reaction, Microp. Mesop. Mater. 29 (1999) 191-203.

[16] A.T. Aguayo, A.G. Gayubo, R. Vivanco, M. Olazar, J. Bilbao, Role of acidity and microporous structure in alternative catalysts for the transformation of methanol into olefins, Appl. Catal. A 283 (2005) 197-207.

[17] P. Tian, Y. Wei, M. Ye, Z. Liu, Methanol to olefins (MTO): From fundamentals to commercialization, ACS Catal. 5 (2015) 1922-1938.

[18] S. Müller, Y. Liu, M. Vishnuvarthan, X. Sun, A.C. Van Veen, G.L. Haller, M. Sanchez-Sanchez, J.A. Lercher, Coke formation and deactivation pathways on H-ZSM-5 in the conversion of methanol to olefins, J Catal. 325 (2015) 48-59.

[19] F.L. Bleken, K. Barbera, F. Bonino, U. Olsbye, K.P. Lillerud, S. Bordiga, P. Beato, T.V.W. Janssens, S. Svelle, Catalyst deactivation by coke formation in microporous and desilicated zeolite H-ZSM-5 during the conversion of methanol to hydrocarbons, J. Catal. 307 (2013) 62-73.

[20] Y. Hirota, K. Murata, M. Miyamoto, Y. Egashira, N. Nishiyama, Light olefins synthesis from methanol and dimethylether over SAPO-34 nanocrystals, Catal. Lett. 140 (2010) 22-26.

[21] Y. Li, M. Zhang, D. Wang, F. Wei, Y. Wang, Differences in the methanol-to-olefins reaction catalyzed by SAPO-34 with dimethyl ether as reactant, J. Catal. 311 (2014) 281-287.

[22] Y. Hirota, M. Yamada, Y. Uchida, Y. Sakamoto, T. Yokoi, N. Nishiyama, Synthesis of SAPO-18 with low acidic strength and its application in conversion of dimethylether to olefins, Microp. Mesop. Mater. 232 (2016) 65-69.

[23] A.S. Al-Dughaither, H. de Lasa, Neat dimethyl ether conversion to olefins (DTO) over HZSM-5: Effect of SiO_2/Al_2O_3 on porosity, surface chemistry, and reactivity, Fuel 138 (2014) 52-64.

[24] P. Pérez-Uriarte, M. Gamero, A. Ateka, M. Díaz, A.T. Aguayo, J. Bilbao, Effect of the acidity of HZSM-5 zeolite and binder in the DME transformation to olefins, Ind. Eng. Chem. Res. 55 (2016) 1513-1521.

[25] P. Pérez-Uriarte, A. Ateka, M. Gamero, A.T. Aguayo, J. Bilbao, Effect of the operating conditions in the transformation of DME to olefins over a HZSM-5 zeolite catalyst, Ind. Eng. Chem. Res. 55 (2016) 6569-6578.

[26] P. Pérez-Uriarte, A. Ateka, A.T. Aguayo, A.G. Gayubo, J. Bilbao, Kinetic model for the reaction of DME to olefins over a HZSM-5 zeolite catalyst, Chem. Eng. J. 302 (2016) 801-810.

[27] T.R. Forester, R.F. Howe, In situ FTIR studies of methanol and dimethyl ether in ZSM-5, J. Amer. Chem. Soc. 109 (1987) 5076-5082.

[28] H. Yamazaki, H. Shima, H. Imai, T. Yokoi, T. Tatsumi, J.N. Kondo, Direct production of propene from methoxy species and dimethyl ether over H-ZSM-5, J. Phys. Chem. C 116 (2012) 24091-24097.

[29] A.G. Gayubo, A.T. Aguayo, M. Castilla, A.L. Moran, J. Bilbao, Role of water in the kinetic modeling of methanol transformation into hydrocarbons on HZSM-5 zeolite, Chem. Eng. Commun. 191 (2004) 944-967.

[30] A.T. Aguayo, D. Mier, A.G. Gayubo, M. Gamero, J. Bilbao, Kinetics of methanol transformation into hydrocarbons on a HZSM-5 zeolite catalyst at high temperature (400-550 ºC), Ind. Eng. Chem. Res. 49 (2010) 12371-12378.

[31] A.G. Gayubo, A.T. Aguayo, A.L. Morán, M. Olazar, J. Bilbao, Role of water in the kinetic modeling of catalyst deactivation in the MTG process, AIChE J. 48 (2002) 1561-1571.

[32] D. Mier, A.T. Aguayo, A.G. Gayubo, M. Olazar, J. Bilbao, Synergies in the production of olefins by combined cracking of n-butane and methanol on a HZSM-5 zeolite catalyst, Chem. Eng. J. 160 (2010) 760-769.

[33] P.L. Benito, A.G. Gayubo, A.T. Aguayo, M. Castilla, J. Bilbao, Concentration-dependent kinetic model for catalyst deactivation in the MTG process, Ind. Eng. Chem. Res. 35 (1996) 81-89.

[34] A.G. Gayubo, A.T. Aguayo, M. Olazar, R. Vivanco, J. Bilbao, Kinetics of the irreversible deactivation of the HZSM-5 catalyst in the MTO process, Chem. Eng. Sci. 58 (2003) 5239-5249.

[35] A.G. Gayubo, A.T. Aguayo, A. Alonso, J Bilbao, Kinetic modeling of the methanol-to-olefins process on a silicoaluminophosphate (SAPO-18) catalyst by considering deactivation and the formation of individual olefins, Ind. Eng. Chem. Res. 46 (2007) 1981-1989.

[36] D. Mier, A.G. Gayubo, A.T. Aguayo, M. Olazar, J. Bilbao, Olefin production by co-feeding methanol and n-butane. Kinetic modeling considering the deactivation of HZSM-5 Zeolite, AIChE J. 57 (2011) 2841-2853.

[37] A.T. Aguayo, J.M. Arandes, M Olazar, J. Bilbao, Study of temperature-programmed desorption of tert-butylamine to measure the surface acidity of solid catalysts, Ind. Eng. Chem. Res. 29 (1990) 1621-1626.

[38] E. Epelde, A.G. Gayubo, M. Olazar, J. Bilbao, A.T. Aguayo, Modified HZSM-5 zeolites for intensifying propylene production in the transformation of 1-butene, Chem. Eng. J. 251 (2014) 80-91.

[39] Y. Jiang, J. Huang, V.R. Reddy Marthala, Y.S. Ooi, J. Weitkamp, M. Hunger, In situ MAS NMR-UV/Vis investigation of H-SAPO-34 catalysts partially coked in

the methanol-to-olefin conversion under continuous-flow conditions and of their regeneration, Microp. Mesop. Mater. 105 (2007) 132-139.

[40] D. Mores, E. Stavitski, M.H.F. Kox, J. Kornatowski, U. Olsbye, B.M. Wechhuysen, Space- and time-resolved in-situspectroscopy on the coke formation in molecular sieves: Methanol-to-olefin conversion over H-ZSM-5 and H-SAPO-34, Chem - A Europ. J. 14 (2008) 11320-11327.

[41] D.S. Wragg, A. Grønvold, A. Voronov, P. Norby, H. Fjellvåg, Combined XRD and Raman studies of coke found in SAPO-34 after methanol and propene conversion, Microp. Mesop. Mater. 173 (2013) 166-174.

[42] J. Chen, J. Li, Y. Wei, C. Yuan, B. Li, S. Xu, Y. Zhou, J. Wang, M. Zhang, Z. Liu, Spatial confinement effects of cage-type SAPO molecular sieves on product distribution and coke formation in methanol-to-olefin reaction, Catal. Commun. 46 (2014) 36-40.

[43] P.L. Benito, A.G. Gayubo, A.T. Aguayo, M. Olazar, J. Bilbao, Deposition and characteristics of coke over a HZSM5 zeolite based catalyst in the MTG process, Ind. Eng. Chem. Res. 35 (1996) 3991-3998.

[44] B. Valle, P. Castaño, M. Olazar, J. Bilbao, A.G. Gayubo, Deactivating species in the transformation of crude bio-oil with methanol into hydrocarbons on a HZSM-5 catalyst, J. Catal. 285 (2012) 304-314.

[45] A.G. Gayubo, A. Alonso, B. Valle, A.T. Aguayo, J. Bilbao, Kinetic model for the transformation of bioethanol into olefins over a HZSM-5 zeolite treated with alkali, Ind. Eng. Chem. Res. 49 (2010) 10836-10844.

[46] K. Toch, J.W. Thybaut, G.B. Marin, A systematic methodology for kinetic modeling of chemical reactions applied to n-hexane hydroisomerization, AIChE J. 61 (2015) 881-892.

[47] G. Elordi, G. Lopez, M. Olazar, R. Aguado, J. Bilbao, Product distribution modelling in the thermal pyrolysis of high density polyethylene, J. Hazard. Mater. 144 (2007) 708-714.

[48] D. Mier, A.T. Aguayo, M. Gamero, A.G. Gayubo, J. Bilbao, Kinetic modeling of n-butane cracking on HZSM-5 zeolite catalyst, Ind. Eng. Chem. Res. 49 (2010) 8415-8423.

[49] G. Elordi, M. Olazar, G. Lopez, P. Castaño, J. Bilbao, Role of pore structure in the deactivation of zeolites (HZSM-5, Hβ and HY) by coke in the pyrolysis of polyethylene in a conical spouted bed reactor, Appl. Catal. B 102 (2011) 224-231.

[50] J. Corella, J. Adanez, A. Monzon, Some intrinsic kinetic equations and deactivation mechanisms leading to deactivation curves with a residual activity, Ind. Eng. Chem. Res. 27 (1988) 375-381.

[51] A. Borgna, T.T. Garetto, A. Monzon, C.R. Apesteguia, Deactivation model with residual activity to study thioresistance and thiotolerance of naphtha reforming catalysts, J. Catal. 146 (1994) 69-81.

[52] A. Monzon, E. Romero, A. Borgna, Relationship between the kinetic parameters of different catalyst deactivation models, Chem. Eng. J. 94 (2003) 19-28.

[53] E. Epelde, A.T. Aguayo, M. Olazar, J. Bilbao, A.G. Gayubo, Kinetic model for the transformation of 1-butene on a K-modified HZSM-5 catalyst, Ind. Eng. Chem. Res. 53 (2014) 10599-10607.

Supplementary information

DEACTIVATION KINETICS FOR THE CONVERSION OF DIMETHYL ETHER TO OLEFINS OVER A HZSM-5 ZEOLITE CATALYST

Paula Pérez-Uriarte*, Ainara Ateka, Ana G. Gayubo, Tomás Cordero-Lanzac, Andrés T. Aguayo, Javier Bilbao

Department of Chemical Eng., University of the Basque Country (UPV/EHU). P.O. Box 644, 48080. Bilbao (Spain). (*) Corresponding author: paula.perez@ehu.es

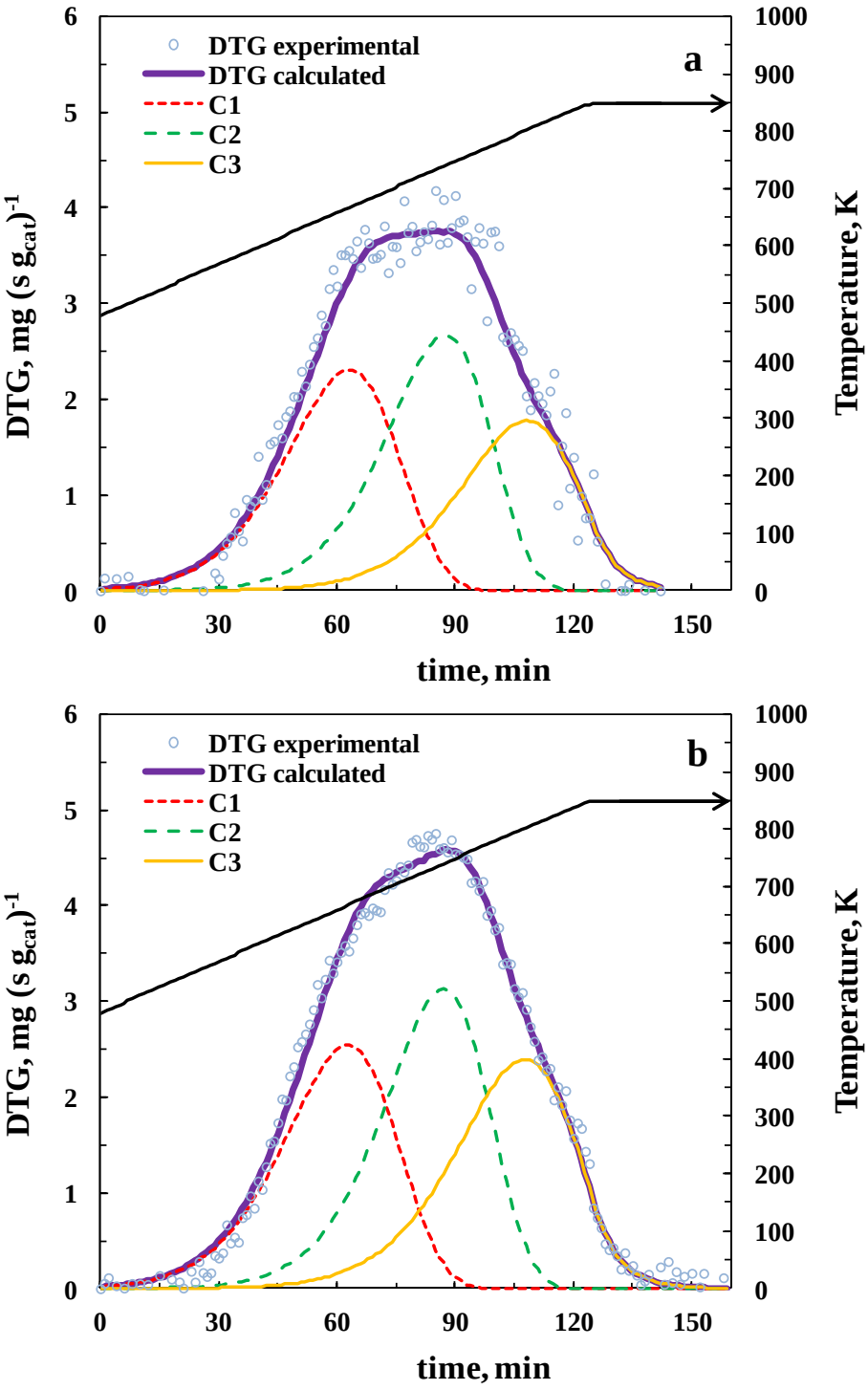

Figure S1. TPO curve deconvolution and identification of three fractions of coke (C1, C2, C3) deposited on the deactivated catalyst. Reaction conditions: space time, 1.5 gcat h mol_C^{-1}; feed, pure DME; time on stream, 18 h; temperature, 598 K (a), 648 K (b) and 673 K (c).

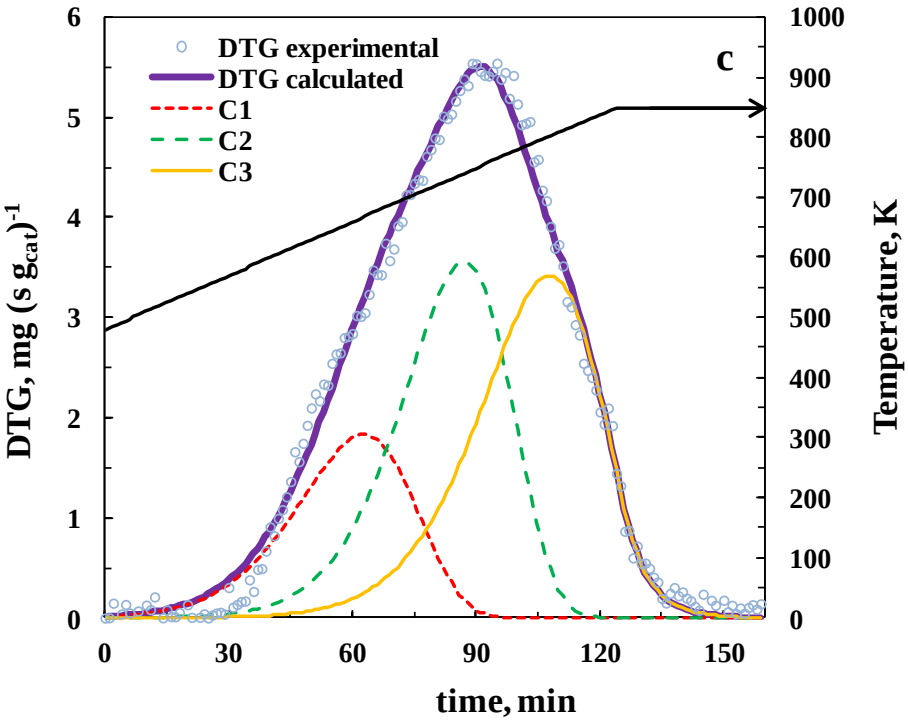

Figure S1. Continuation.